Journal of the European Ceramic Society 21 (2001) 515–522

www.elsevier.com/locate/jeurceramsoc

Synthesis and characterization of $Li_{1+\delta}Mn_{2-\delta}O_4$ powders prepared by citric acid gel process

Y.M. Hon, K.Z. Fung *, M.H. Hon

Department of Materials Science and Engineering, National Cheng Kung University, Tainan 70101, Taiwan

Received 27 November 1999; received in revised form 25 July 2000; accepted 31 July 2000

Abstract

$Li_{1+\delta}Mn_{2-\delta}O_4$ were synthesized by citric acid gel process using lithium acetate and manganese acetate as the sources of lithium and manganese. Spinel $Li_{1+\delta}Mn_{2-\delta}O_4$ had been synthesized at various temperatures from 200 to 500°C and the synthesis mechanism was examined by thermal and structural analysis. $Li_{1+\delta}Mn_{2-\delta}O_4$ can be synthesized as low as 200°C is attributed to the short distance between lithium and manganese formed in precursor prepared by citric acid gel process . Thus, lithium and manganese could react each other and form the desired compound at low temperatures. The lattice parameter of powders increased with increasing temperature from 8.136 Å at 200°C to 8.211 Å at 500°C. The specific surface area of sample calcined at 200°C was 160 m^2/g and deceased with calcination temperature increasing. From the SEM studies, the powder prepared at 200°C showed porous structure due to the liberation of CO_2 and H_2O from the decomposition of organic material. The particle size of powder calcined at 300°C for 24 h in the range of 60 to 85 nm. The powder synthesized by citric acid gel process showed circular shape and did coarsen significantly with the calcination temperature increased.

Keywords: Batteries; $LiMn_2O_4$; Powders-chemical preparation; Sol-gel processes

1. Introduction

Lithium manganese oxides have received a great deal of interest toke used as lithium insertion electrodes for rechargeable lithium batteries. These materials are capable providing high cell voltage, good rechargeability and a wide operation temperature range with much lower cost and no toxicity compared to $LiCoO_2$ and $LiNiO_2$.[1–4]

Lithium manganese oxides exhibit AB_2O_4 spinel structure when synthesized in oxidizing environment. The concept of using the $[B_2]O_4$ framework of an $A[B_2]O_4$ spinel, where A and B refer to cations in tetrahedral and octahedral sites, respectively, as an insertion electrode for lithium batteries was demonstrated several years ago.[5] Particular attention has been given to the $LiMn_2O_4$, $Li_2Mn_4O_9$ and $Li_4Mn_5O_{12}$ in Li–Mn–O system.[6–11] The best-known lithium manganese oxide is $LiMn_2O_4$ that has a space group symmetry of Fd3m. In $Li[Mn_2]O_4$, the lithium ions occupy the tetrahedral 8a sites and the manganese ions are located at the octahedral 16d sites. The oxygen ions, which are cubic-closest packed, occupy the 32e positions.[6]

Electrochemical extraction of lithium from $Li[Mn_2]O_4$ occurs in two stages at approximately 2.9 and 4 V.[6] The undesired Jahn–Teller distortion can be avoided by introducing additional Li-ions at 16d sites in order to keep the average Mn-oxidation above 3.5. Additional Li-ions at the 16d sites will, however, decrease the capacity.

It is the current consensus that a wide range of solid solution exists within the Li–Mn–O family of spinel compounds and the composition of the spinel electrode plays a very important role in controlling the rechargeability of the electrode.[12–14] Therefore, attention should be paid to the control of the material synthesis process in order to obtain single-phase compounds with desired stoichiometry.

It has been reported that the $LiMn_2O_4$ powder prepared at high temperatures using solid state reaction degrades rapidly upon cycling although the initial capacity is satisfactory.[2] Recently, solution techniques have been widely used to synthesize $LiMn_2O_4$ powder. Solution technique provides the advantages of homogeneous mixing, lower synthesizing temperature and high specific surface area. The chemical diffusion coefficient

* Corresponding author. Tel.: +886-6-238-0208; fax: +886-6-238-0208.

E-mail address: kzfung@mail.ncku.edu.tw (K.Z. Fung).

0955-2219/01/$ - see front matter
PII: S0955-2219(00)00217-X

in $LiMn_2O_4$ samples processed at lower temperature is apparently higher than that in samples calcined at higher temperature.[15]

In recent years, several low temperature synthesis techniques such as precipitation,[16] sol-gel[17] and pechini[18] processes have been developed. The organic acid gel process was also developed to fabricate fine ceramic powders such as $NiFe_2O_4$, superconductor, $BaTiO_3$, $LiMn_2O_4$, etc.[19–21] There are two main advantages of using organic acid gel process to synthesize lithium manganese oxide powder: (1) This synthesis process makes route particularly attractive for high specific surface area and easy controlling in the ratio of lithium to manganese at low temperatures. (2) All synthesis procedure can be carried out in air unlike some sol-gel processes, which require an inert atmosphere. In this study, lithium manganese oxides were synthesized by citric acid gel process using lithium acetate and manganese acetate as the sources of lithium and manganese.

Thus, the objective of this work was to investigate the effect of the calcination temperature on the phase transition, purity, morphology and specific surface area of lithium manganese oxide powders. The electrical conductivity and electrochemical behavior of cathode material synthesized by this process will be discussed in later publications.

2. Experimental

2.1. Optimization of precursor

2.1.1. Citric acid gel process

Lithium manganese oxide powders were prepared by citric acid gel process. Lithium acetate (98% purity, Aldrich) and manganese acetate (99% purity, Showa Chemicals Inc.) used as the sources of lithium and manganese were dissolved in ethanol, the molar ratio of metal ions Li^+: Mn^{2+} being 1:2. The metal-ion ethanol solution was then mixed with an ethanol solution of citric acid (99.5% purity, Ferak). During mixing, the solution abruptly transformed into a viscous gel. The final gel contained 0.025 M Li^+, 0.05 M Mn^{2+} and 0.1 M citric acid. The gel was heated at 80°C to remove the ethanol. After drying, the dried powder was obtained and used as the lithium-manganese-citrate precursor. The precursor was heated at 200°C for 6 h, followed by the calcination process at temperatures ranging from 200 to 500°C for 24 h. Finally, the calcined powders were furnace-cooled to room temperature.

2.1.2. Thermal analysis

Thermal analysis was conducted to examine the possible heat and weight changes during the heating and calcination processes. Thermal analysis was carried out using differential thermal analyzer and thermogravimetric analysis (DTA/TG, Setaram Company TAG 24) between 25 and 600°C with a heating rate of 2°C/min in air to investigate the possible phase transformation.

2.2. Powder characterization

2.2.1. Crystallographic and chemical analysis

The phase identity, crystal structure, and lattice constants of the materials were investigated using Rigaku X-ray diffractometer (XRD) with the CuK_α radiation at 30 kV, 20 mA. XRD data were collected between 10 and 70° of 2θ angles with a step interval of 0.01°. Lattice constants were determined by a least-squares refinement of the d-spacing, which were measured in comparison with an internal standard of pure Si. The content of lithium and manganese in the samples calcined at various temperatures was analyzed by Atomic-Absorption Spectroscopy (AAS, Hitachi Z-8200). The average valence was determined by titration method. About 0.06 g of the sample was dissolved in 20 ml of an acidified 0.0849 M Fe(II) solution. During dissolution higher Mn oxidation states (III) and (IV) are reduced to Mn(II) by the oxidation of Fe(II) to Fe(III). The excess Fe(II) is back titrated with 0.02 M $KMnO_4$.

2.2.2. Morphology and specific surface area characterization

Scanning electron microscope (SEM; Philips XL-40FEG) was used to examine the particle size and morphology of synthesized powders. The specific surface area of lithium manganese oxide powders was measured using Gemini 2360 surface area analyzer based on the BET process.

3. Results and Discussion

3.1. Thermal analysis and phase identification

The TG/DTA analysis was conducted on citric acid, lithium manganese citrate, lithium citrate and manganese citrate, respectively.

3.1.1. Citric acid

The TG-DTA analysis was first conducted on pure citric acid at a heating rate of 2°C/min, as shown in Fig. 1(a). The TG curve shows about 90% weight loss occurring at temperatures between 200 and 300°C which correlated with a strong DTA endothermic peak representing the decomposition of a complex manner. The complex reaction caused by the possible stepwise decomposition of citric acid has been proposed by Eype.[22] The possible reaction is shown as what follows:

$$\text{citric acid} \xrightarrow{175^\circ C} \text{aconitic acid } (C_6H_6O_6) + H_2O_{(g)};$$

$$\text{aconitic acid} \xrightarrow{\text{heat}} \text{itaconic acid } (C_5H_6O_4) + CO_{2(g)}$$

$$\text{itaconic acid} \xrightarrow{\text{heat}} \text{itaconic anhydride } (C_5H_4O_3) + H_2O,$$
$$\text{or acetone-dicarboxylic acid } \left(CO(CH_2 \cdot COOH)_2\right)$$

Finally, a minor weight loss was observed between 385 and 450°C which can be correlated to the strong DTA exothermic peak at the same temperature range due to the combustion of either citric acid derivations or residual carbon.

3.1.2. Lithium manganese citrate

Fig. 1(b) shows the TG and DTA curves of the lithium manganese citrate precursor. The curves show that weight loss began at 150°C. An abrupt weight loss was observed at 244°C accompanied by a sharp exothermic reaction. At temperatures higher than 280°C, there was no further weight loss and heat variations on TG/DTA curves. Traces of XRD for powders calcined at 200°C for 15 min, is shown in Fig 2(a), and no diffraction peak was found. The XRD trace of crystallized lithium manganese oxide formed after heat treatment at 280°C for 15 min, is shown in Fig. 2(b). Thus, the TG/DTA curves in Fig. 1(b) show very important information: lithium manganese oxide compounds were synthesized acutely at 244°C. At temperatures higher than 280°C, organic materials decomposed completely.

In contrast to our results where a single exothermic peak is observed in the DTA trace (heating rate 2°C/min), the results of Tsumura[19] showed that there were exothermic peaks at 180, 253 and 298°C, and Prabaharan[20] showed single exothermic peak at 238°C. Tsumura ascribed that the exothermic peak at 250°C combined with XRD data was caused by the formation of $LiMn_2O_4$; another exothermic peak at 290°C was due to the probable combustion of organic component. Prabaharan ascribed the single exothermic peak at 238°C due to the formation of $LiMn_2O_4$ accompanied by the decomposition of organic groups. Based on the results of the present work, it was found that there is no weight loss after the sharp exothermic peak. Similar results were also found on Tsumura and Prabaharan's work. These results indicated that the sharp exothermic

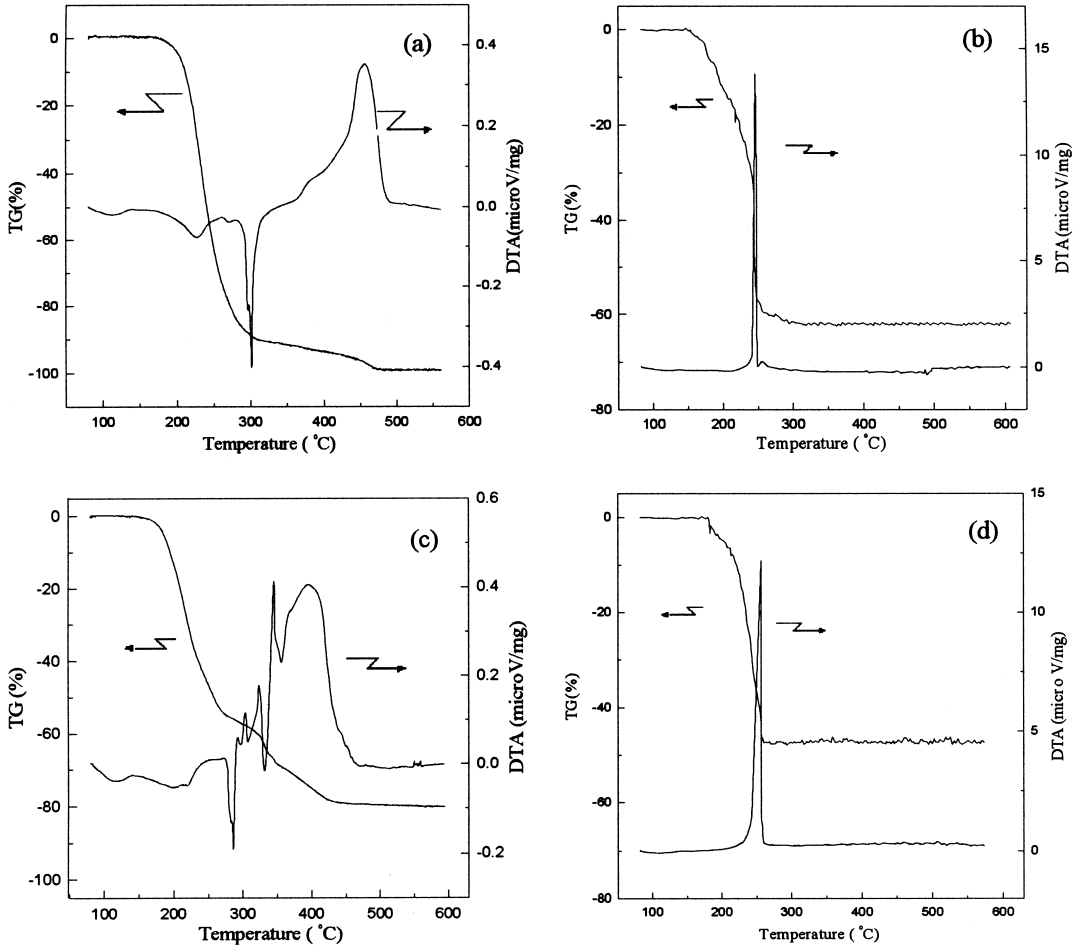

Fig. 1. TG-DTA analysis for (a) citric acid, (b) lithium manganese citrate, (c) lithium citrate, (d) manganese citrate at a heating rate of 2°C/min in air.

peak at 244°C resulted be from the combustion of organic derivation and the released heat further enhanced the formation of lithium manganese oxides.

In order to understand the decomposition of lithium manganese citrate precursor in detail, lithium citrate and manganese citrate precursors were prepared individually and characterized by TG/DTA and XRD. Fig. 1(c) and (d) showed the TG/DTA curves of lithium citrate and manganese citrate precursors at a heating rate of 2°C/min in air, respectively.

3.1.3. Lithium citrate

In comparison with the results of citric acid, the TG/DTA analysis on the lithium citrate precursor shows three extra exothermic peaks between 290 and 350°C. Fig. 3 shows the XRD patterns of lithium citrate precursors calcined at various temperatures from 300 to 500°C for 10 min. The $C_{15}H_{16}O_2$ and Li_2CO_3 compounds were formed at 300°C. At 500°C, $C_{15}H_{16}O_2$ decomposed and all peaks correspond to the monoclinic structure of Li_2CO_3.

3.1.4. Manganese citrate

The TG/DTA curves for manganese citrate precursor is shown in Fig. 1(d). A exothermic peak at 250°C of manganese citrate which is very close to that of lithium manganese citrate at 244°C, as shown in Fig. 1(b). This result indicates that the formation of $Li_{1+\delta}Mn_{2-\delta}O_4$ from lithium manganese citrate is strongly related to the exothermic reaction of manganese citrate. The significance of manganese citrate on the formation of $Li_{1+\delta}Mn_{2-\delta}O_4$ will be discussed in the later section.

Fig. 4 shows the XRD patterns of manganese citrate precursor calcined at 200 and 500°C for 1 h. The result shows that crystalline γ-Mn_3O_4 formed at 200°C and transformed to Mn_2O_3 with a orthorhombic structure at higher temperatures.

3.2. Effect of lithium citrate and manganese citrate on the formation of $Li_{1+\delta}Mn_{2-\delta}O_4$

The thermal and structure analysis in Fig. 1(a)–(d), it showed that TG/DTA and XRD traces for lithium citrate did not match with those for lithium manganese

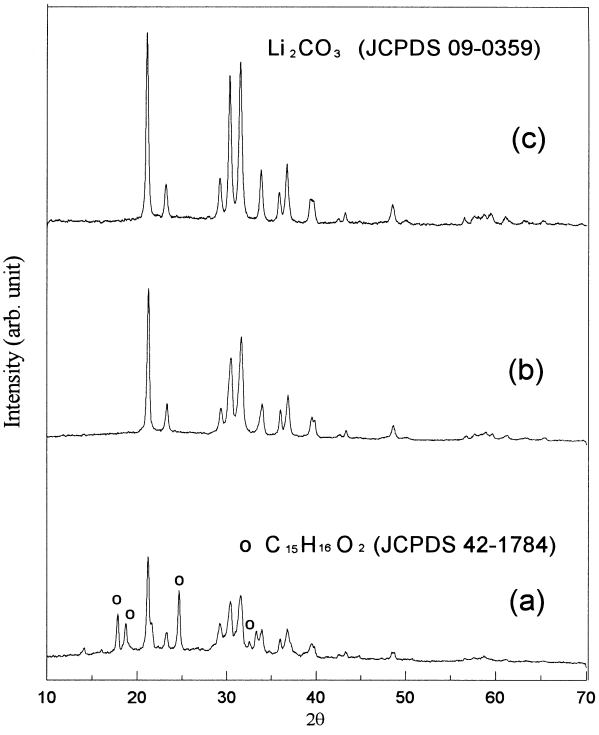

Fig. 3. The XRD patterns of lithium citrate precursor calcined at (a) 300°C, (b) 400°C, (c) 500°C for 10 min.

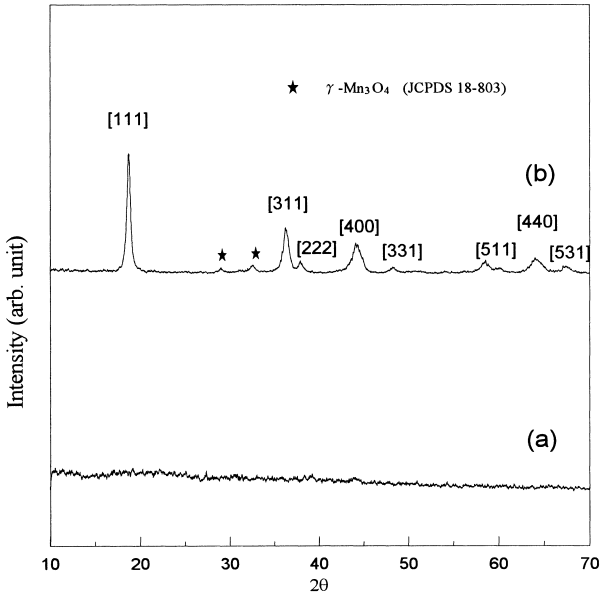

Fig. 2. The XRD patterns of lithium manganese oxide synthesized at (a) 200°C, (b) 280°C for 15 min.

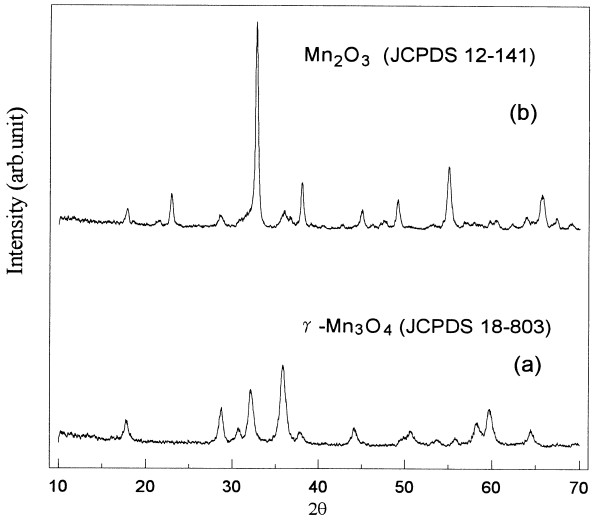

Fig. 4. The XRD patterns of manganese citrate precursor calcined at (a) 200°C, (b) 500°C for 1 h.

oxide precursors. This result indicates that lithium ions were uniformly distributed in the solution and all lithium ions were consumed during the formation of lithium manganese oxide. On the other hand, the TG/DTA traces for both manganese citrate and lithium manganese citrate are very similar. Combined with the results of XRD, it is suggested that the formation of $Li_{1+\delta}Mn_{2-\delta}O_4$ be greatly enhanced by the exothermic reaction of manganese citrate. When lithium manganese citrate precursors were heated, a portion of aggregated manganese citrate reacted with oxygen and formed γ-Mn_3O_4 as the impurity phase at low temperature. Lithium ions, however, did not precipitate as the impurity but remained in the solution uniformly. Furthermore, the large amount of heat was released during the oxidation of manganese citrate precursor at 244°C and triggered the formation of lithium manganese oxide. From the result of TG/DSC and XRD, it is believed that the lithium and manganese ions were homogeneously trapped on an atomic scale. When the precursor was formed. The lithium manganese oxide formed immediately when the heat was released from the organic materials. If the lithium and manganese ions are trapped unhomogeneously on an atomic scale and aggregate in precursor, the Li_2CO_3 and manganese oxides must formed at low temperature then reacted to lithium manganese oxides at higher temperature.

3.3. Isothermal treatment of lithium manganese citrate

As described in the previous section, $Li_{1+\delta}Mn_{2-\delta}O_4$ was formed at 244°C from the TG/DTA curves. In order to verify the possibility of obtaining lithium manganese oxide at temperatures lower than 244°C, isothermal analysis of lithium manganese citrate precursors at 200°C was conducted. DTA and XRD traces for the lithium manganese citrate precursor synthesized at 200°C for various periods of time are shown in Figs. 5 and 6. From the result of DTA analysis, a broaden exothermic peak appeared after calcining at 200°C for 3 h (10800 s) which attributed to the formation of $Li_{1+\delta}Mn_{2-\delta}O_4$. In Fig. 6, the precursor and calcination at 200°C for 1.5 h are amorphous structure. After calcining at 200°C for 3 and 6 h, $Li_{1+\delta}Mn_{2-\delta}O_4$ formed with small amount of second phase, γ-Mn_3O_4. The impurity phase, γ-Mn_3O_4, disappeared with the calcination time increased to 30 h. From the result of XRD, it was found that the time of formation of $Li_{1+\delta}Mn_{2-\delta}O_4$ was consisting to the result of DTA analysis, was shown in Fig. 5. This result clearly shows that $Li_{1+\delta}Mn_{2-\delta}O_4$ was able to form at temperatures as low as 200°C by citric acid gel process. $Li_{1+\delta}Mn_{2-\delta}O_4$ can be synthesized as such a low temperature is attributed to the short distance between lithium and manganese elements in precursor formed by this process. Thus, elements can easily react each other and form the compound at low temperature. However, longer calcination time at low temperature is expected to obtain a well-crystallized compound.

3.4. Evaluation of $Li_{1+\delta}Mn_{2-\delta}O_4$

The XRD pattern of a precursor after heated at 200°C for 24 h is given in Fig. 7(a). Apparently, $Li_{1+\delta}Mn_{2-\delta}O_4$ with spinel structure was formed after heating at this relatively low temperature. The XRD

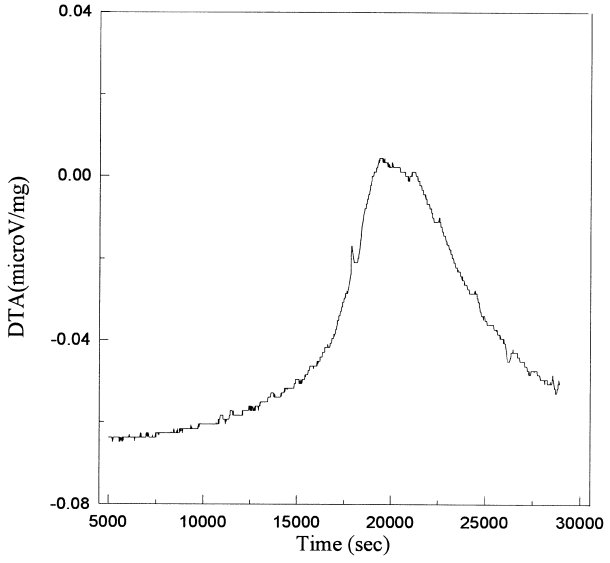

Fig. 5. DTA analysis for lithium manganese citrate precursor heated at 200°C for various periods of time.

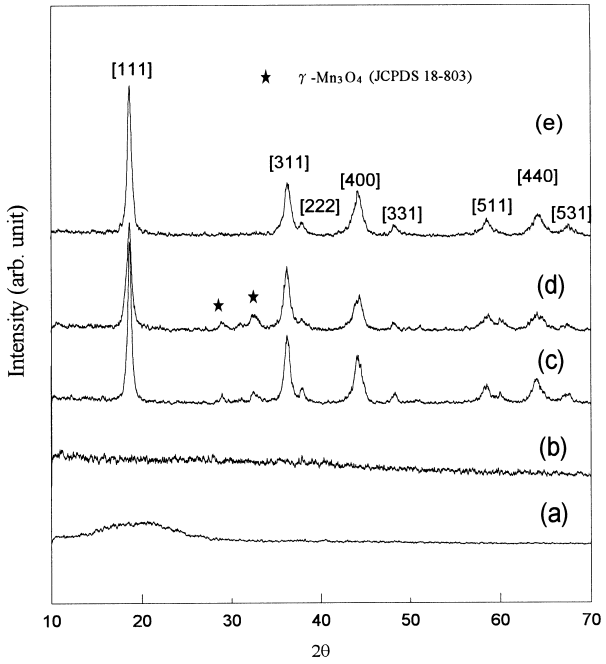

Fig. 6. The XRD patterns of lithium manganese oxide calcined at 200°C for (a) 0 h (precursor), (b) 1.5 h, (c) 3 h, (d) 6 h, (e) 30 h in air.

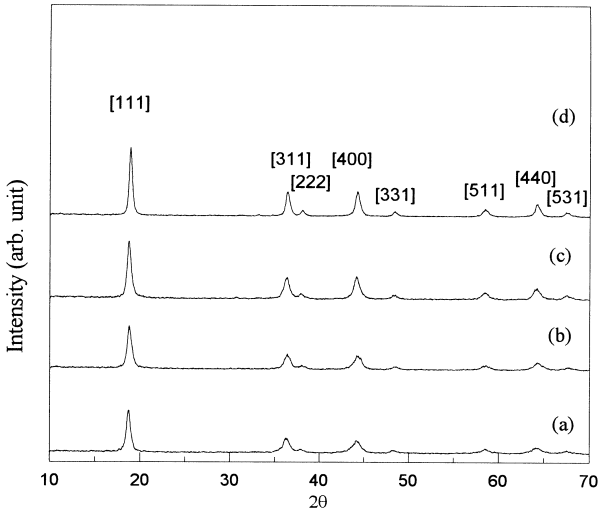

Fig. 7. The XRD patterns of lithium manganese oxide synthesized at (a) 200°C, (b) 300°C, (c) 400°C, (d) 500°C for 24 h.

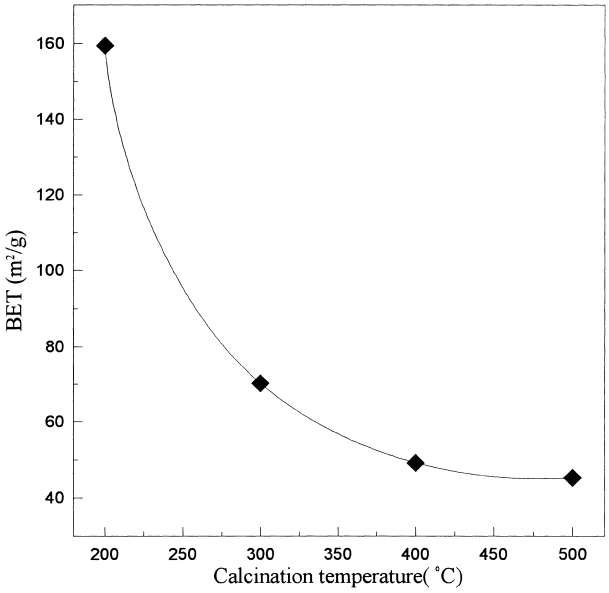

Fig. 8. Effect of the calcination temperature on the specific surface area of the lithium manganese oxides prepared by citric acid gel process.

pattern also shows broader peaks at high scattering angles. The XRD powder pattern obtained from a precursor after heated at 300 and 400°C for 24 h were presented in Figs. 7(b) and (c). The pattern is almost the same as that in Fig. 7(a) except that the peak widths are narrower. The XRD pattern of a precursor heat treated at 500°C for 24 h is shown in Fig. 7(d). The sharp diffraction reflections indicate a well-crystallized spinel structure.

The lattice constant (a) and chemical formula of spinel $Li_{1+\delta}Mn_{2-\delta}O_4$ powders, obtained by indexing the XRD peaks using a least-squares programs and chemical analysis, was showed in Table 1. The lattice parameter increases with increasing calcination temperature from 8.136 Å (at 200°C) to 8.211 Å at (500°C). Following reasons causes the change in lattice parameter. Firstly, the defect concentration decreased with increasing calcination temperature increased. Secondly, lower-temperature calcination factors the formation of higher valence Mn ions, which enhance the formation of cation deficiencies are created for the charge compensation. For example, MnO_2 with all Mn^{4+} transforms progressively to Mn_2O_3 with all Mn^{3+} for the binary manganese oxide system as the temperature increase. The atomic radius of Mn^{4+} (0.67 Å) is smaller than that of Mn^{3+} (0.72 Å) and thus the lattice constant of spinel $Li_{1+\delta}Mn_{2-\delta}O_4$ obtained at lower temperatures shows smaller value than that of the spinel $Li_{1+\delta}Mn_{2-\delta}O_4$ synthesized at higher temperatures.

3.5. Specific surface area and morphology

The dependence of the specific surface area on the calcination temperature of synthesized process is shown in Fig. 8. It can be seen that the specific surface area decreases abruptly with increasing calcination temperature. As temperatures greater than 400°C, the specific surface area of synthesized powder decreases slowly. The specific surface area of the powder calcined at 200°C for 24 h was 160 m^2/g then quickly decreased to 49 m^2/g as the temperature increased to 400°C. This result is attributed to the large amount of heat released from the combustion of citric acid at about 244°C that caused the agglomeration and growth of fine particles.

Fig. 9 shows the SEM micrographs of $Li_{1+\delta}Mn_{2-\delta}O_4$ powder calcined at various temperatures. The morphology of powder calcined at 200°C shows very porous structure, as shown in Fig. 9(a). Formation of large particle was attributed to highly viscous citric acid, enhanced the aggregation of powder during decomposition

Table 1
Lattice constant and chemical analysis of $Li_{1+\delta}Mn_{2-\delta}O_4$ calcined at different temperatures

Temperature (°C)	Lattice parameter (a, Å)	Content of Li (wt.%)	Content of Mn (wt.%)	Average valence Mn	Chemical formula
200	8.136	3.63	56.5	3.69	$Li_{0.97}Mn_{1.90}O_4$
300	8.152	3.72	57.4	3.67	$Li_{0.98}Mn_{1.91}O_4$
400	8.188	3.74	56.8	3.66	$Li_{1\ 00}Mn_{1.91}O_4$
500	8.211	3.71	56.9	3.62	$Li_{1.00}Mn_{1.94}O_4$

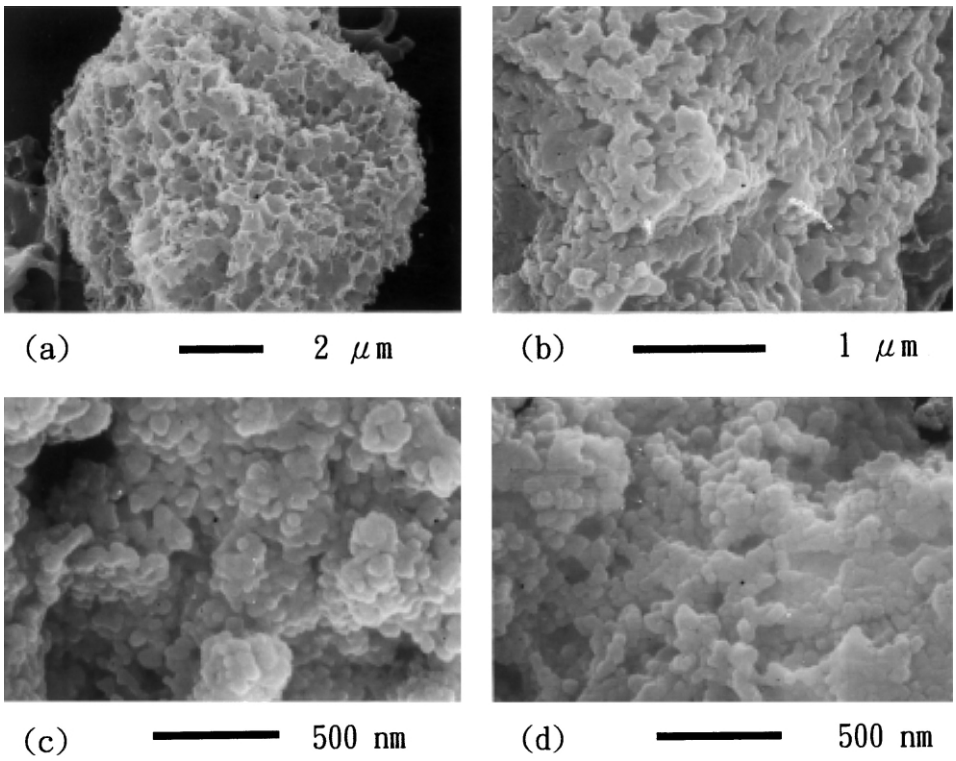

Fig. 9. SEM micrographs of lithium manganese oxides prepared by citric acid gel method at: (a) 200°C, (b) 200°C, (c) 300°C, (d) 500°C for 24 h.

process. The porous structure was caused by the liberation of CO_2 and H_2O from the decomposition of citric acid, which formed the connected hollow channels. Fig. 9(b) shows that the average particle size of powder calcined at 300°C for 24 h falls in a narrow rang between 60 and 85 nm. As the calcination increased to 500°C, the particle size remained unchanged. Thus, the $Li_{1+\delta}Mn_{2-\delta}O_4$ powders synthesized by citric acid gel process provide very fine and uniform powder in nanometer range whereas larger and more agglomerated particles with scattered size and shape distributions were usually formed from solid state reactions. The advantage of small particle size is the ability to provided larger surface area and shorter diffusion distance for lithium intercalation and de-intercalation reaction.

4. Conclusion

In the present study, the synthesis of $Li_{1+\delta}Mn_{2-\delta}O_4$ by citric acid gel process was investigated. The phase transformation, specific surface area, morphology and chemical compositions of spinel $Li_{1+\delta}Mn_{2-\delta}O_4$ powder have been systematically characterized as a function of calcination temperature in this work. It was seen that as the calcination temperature increased, the lattice constant increased whereas the average oxidation state of manganese decreased. It is inferred that ah higher calcination temperatures the average oxidation state of manganese becomes smaller and hence the lattice constant of the cubic unit cell of the spinel $Li_{1+\delta}Mn_{2-\delta}O_4$ increased, resulting in lower cation vacancies. $Li_{1+\delta}Mn_{2-\delta}O_4$ powder with well crystallization and 160 m^2/g specific surface area can be synthesized at temperatures as low as 200°C for 24 h, the lowest temperature and highest specific surface area reported so far by citric acid gel process.

Acknowledgements

This work was financially supported by the National Science Council of Taiwan, Grant No. NSC 88-2216-E-006-027, which is gratefully acknowledged.

References

1. Manthiram, A., Electrode materials for rechargeable lithium batteries. *JOM*, 1997, **49**(3), 43–46.
2. Tarascon, J. M., McKinnon, W. R., Coowar, F., Bowmer, T. N., Amatucci, G. and Guyomard, D., Synthesis conditions and oxygen stoichiometry effects on Li insertion into the spinel $LiMn_2O_4$. *J. Electrochem. Soc.*, 1994, **141**(6), 1421–1431.
3. Tarascon, J. M. and Guyomard, D., The $Li_{1+x}Mn_2O_4$/C rocking-chair system: a review. *Electrochimica Acta*, 1993, **38**(9), 1221–1231.
4. Xia, Y., Takeshige, H., Noguchi, H. and Yoshio, M., Studies on an Li–Mn–O spinel system (obtained by melt-impregnation) as a

cathode for 4 V lithium batteries, part 1. Synthesis and electrochemical behaviour of $Li_xMn_2O_4$. *J. Power Sources*, 1995, **56**, 61–67.
5. Thackeray, M. M., David, W. I. F., Bruce, P. G. and Goodenough, J. B., Lithium insertion into manganese spinels. *Mater. Res. Bull.*, 1983, **18**, 461–472.
6. Thackeray, M. M. and de Kock, A., Synthesis and structural characterization of defect spinels in the lithium–manganese–oxide system. *Mater. Res. Bull.*, 1993, **28**, 1041–1049.
7. de Kock, A., Rossouw, M. H., de Picciotto, L. A., Thackeray, M. M., David, W. I. F. and Ibberson, R. M., Defect spinels in the system $Li_2O{\cdot}yMnO_2$ ($y > 2.5$): a neutron-diffraction study and electrochemical characterization of $Li_2Mn_4O_9$. *Mater. Res. Bull.*, 1990, **25**, 657–664.
8. Rossouw, M. H., de Kock, A., de Picciotto, L. A., Thackeray, M. M., David, W. I. F. and Ibberson, R. M., Structural aspect of lithium–manganese oxide electrodes for rechargeable lithium batteries. *Mater. Res. Bull.*, 1990, **25**, 173–182.
9. Thackeray, M. M., Rossouw, M. H., Kock, A.de and Harpe, A. P.de.La., The versatility of MnO_2 for lithium battery applications. *J. Power Sources*, 1993, **43-44**, 289–300.
10. Takada, T. and Akiba, E., Structure refinement of $Li_4Mn_5O_{12}$ with neutron and X-ray power diffraction data. *J. Solid State Chem.*, 1997, **130**, 74–80.
11. Thackeray, M. M., Kock, A.de, Rossouw, M. H. and Liles, D., Spinel electrodes from the Li–Mn–O system for rechargeable lithium battery applications. *J. Electrochem. Soc.*, 1992, **139**(2), 363–366.
12. David, W. I. F., Thackeray, M. M., Picciotto, L. A.de and Goodenough, J. B., Structure refinement of the spinel-related phases $Li_2Mn_2O_4$ and $Li_{0.2}Mn_2O_4$. *J. Solid State Chem.*, 1987, **67**, 316–323.
13. Yamada, A., Miura, K., Hinokuma, K. and Tanaka, M., Synthesis and structural aspects of $LiMn_2O_{4\pm\delta}$ as a cathode for rechargeable lithium batteries. *J. Electrochem. Soc.*, 1995, **142**(7), 2149–2156.
14. Gummow, R. J., Kock, A.de and Thackeray, M. M., Improved capacity retention in rechargeable 4 V lithium/lithium-manganese oxide (spinel) cells. *Solid State Ionics*, 1994, **69**, 59–67.
15. Chen, L., Huang, X., Kelder, E. and Schoonman, J., Diffusion enhancement in $Li_xMn_2O_4$. *Solid State Ionics*, 1996, **76**, 91–96.
16. Barboux, P., Tarascon, J. M. and Shokoohi, F. K., The use of acetates as precursors for the low-temperature synthesis of $LiMn_2O_4$ and $LiCoO_2$ intercalation compounds. *J. Solid State Chem.*, 1991, **94**, 185–196.
17. Kakihana, M., Sol-gel preparation of high temperature superconducting oxides. *J. Sol-Gel Science and Technology*, 1996, **6**, 7–55.
18. Liu, W., Farrington, G. C., Chaput, F. and Dunn, B., Synthesis and electrochemical studies of spinel phase $LiMn_2O_4$ cathode materials prepared by the pechini process. *J. Electrochem. Soc.*, 1996, **143**(3), 879–884.
19. Tsumura, T., Shimizu, A. and Inagaki, M., Synthesis of $LiMn_2O_4$ spinel via tartrates. *J. Mater. Chem.*, 1993, **3**, 995–996.
20. Sahaya Prabaharan, S. R., Siluvai Michael, M., Prem Kumar, T., Mani, A., Athinarayanasway, K. and Gangadharan, R., Bulk Synthesis of submicrometer powders $LiMn_2O_4$ for secondary lithium batteries. *J. Mater. Chem.*, 1995, **5**, 1035–1037.
21. Hon, Y. M., Fung, K. Z. and Hon, M. H., Effect of temperature and atmosphere on phase stability and morphology of $LiMn_2O_4$ powder synthesized by citric acid gel process. *J. Ceram. Soc. Jpn*, 2000, **108**(5), 462–468.
22. Eype, Spottiswoode, *Dictionary of Organic Compounds*, Oxford University Press, New York, 1965, p. 715.